Politecnico di Torino

Porto Institutional Repository

[Article] Axiomatic/asymptotic technique applied to refined theories for piezoelectric plates

(Article begins on next page)
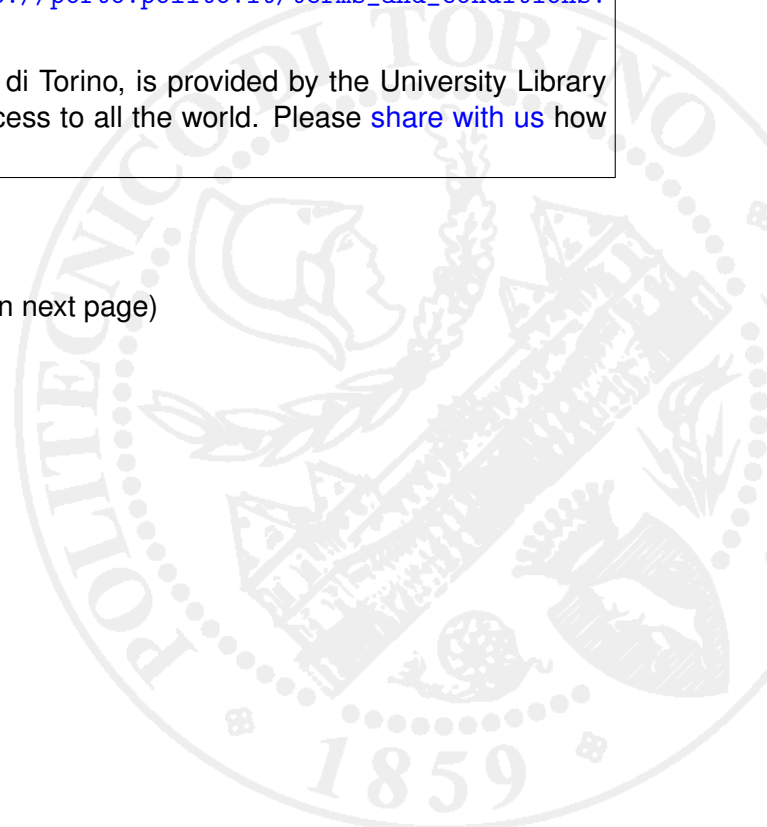
Axiomatic/asymptotic technique applied to refined theories for piezoelectric plates

Maria Cinefra[1], Alessandro Lamberti[1], Ashraf M. Zenkour[2] and Erasmo Carrera[1,2]

(1) Department of Mechanical and Aerospace Engineering,
Politecnico di Torino, Italy
(2) Department of Mathematics, Faculty of Science, King Abdulaziz University,
P.O. Box 80203, Jeddah 21589, Saudi Arabia

Author for correspondence:

E. Carrera, professor,
Department of Mechanical and Aerospace Engineering,
Politecnico di Torino,
Corso Duca degli Abruzzi 24,
10129 Torino, Italy,
tel: +39 011 090 6871,
fax: +39 011 090 6899,
e-mail: alessandro.lamberti@polito.it,
website: www.mul2.com

Abstract

This paper is devoted to the evaluation of refined theories for static response analysis of piezoelectric plate. The Carrera Unified Formulation (CUF) is employed to generate the refined plate models. The CUF allows the hierarchical implementation of refined models based on any-order expressions of the unknown variables. Equivalent Single Layer (ESL) and Layer Wise (LW) approaches are used to generate the refined models. The governing equations are obtained considering Navier-type, closed-form solutions. The axiomatic/asymptotic technique is employed in order to evaluate the relevance of each model term. This technique computes the relevance of a model term by measuring the error introduced with its deactivation with respect to a reference solution. The axiomatic/asymptotic technique is applied considering the sensor and actuator configurations for piezoelectric plates. Moreover, the analyses are performed taking into account the influence of the length-to-thickness ratio (a/h) and the use of isotropic or orthotropic materials. "Best" models are proposed and the stress/displacement components and electric potential distributions are evaluated by means of these reduced models.

1   Introduction

Piezoelectric materials when subjected to a mechanical load generate a positive or negative charge distribution. This phenomenon was discovered in 1880-1881 by Curie brothers (Jacques and Pierre Curie, [1]) for some kind of natural crystals. The known materials which exhibit piezoelectric properties are quartz and tourmaline (natural crystals) and some synthetic crystals such as lithium sulfate, and several kinds of polymers and polarized ceramics. The most common piezoelectric materials are the piezoceramic barium titanate (BaTiO$_3$) and piezo lead zirconate titanate (PZT). The piezoelectric phenomenon can be explained in terms of distortion of the crystal lattice. Further details on piezoelectricity can be found in the books [2], [3] and [4].

Piezoelectric materials present direct and inverse effects; the direct effect means the generation of a distribution of charge when the piezoelectric material is subjected to a mechanical load. Inverse effect, instead, means the deformation of the piezoelectric material when a electric potential is applied. Piezoelectricity can be used to create embedded sensors and embedded actuators. The main advantage offered by these configurations is that a continuous structural health monitoring is possible and hingless mechanisms can be created. This kind of solution is called *smart structure* and a rigorous definition was proposed in [5]:

> A system or material which has built-in or intrinsic sensor(s), actuator(s) and control mechanism(s) whereby it is capable of sensing a stimulus, responding to it in a predetermined manner and extent, in a short/appropriate time, and reverting to its original state as soon as the stimulus is removed.

Examples of the use of smart structure in structural health monitoring and as actuators are discussed in [6], [7], [8] and [9]. The creation of a smart-structure presents several critical aspects, such as the manufacturing, the designing and the control. In this work, the attention is restricted to the analysis of the theories that can be used for the electro-mechanical modeling of plates. A mathematical model for a piezo-mechanic plate analysis should be able to consider both mechanic and electric properties. Firstly, an important distinction should be mentioned: Equivalent Single Layer (ESL) and Layer Wise (LW) approaches. An in-depth discussion can be found in the book by Reddy ([10]). The analysis of a multilayered plate/shell can be performed considering it as a single equivalent lamina; in this case, an ESL approach is employed and the number of unknowns is independent of the number of layers of the plate/shell. On the contrary, if a LW approach is employed, the displacement field is assumed independently for each layer and it is a continuous function in the thickness direction; in this case, each layer presents its own unknowns. In both approaches, a 3D continuum problem is reduced to a 2D problem.

A number of mathematical models for piezo-mechanic analysis are available in the scientific literature. In the field of ESL models, classical formulations can be used for piezo-mechanic analysis and some examples can be found in [3] and in [11]. Anyway these models can be ineffective for such analysis since this kind of structures exhibit different mechanical-electrical properties in the thickness direction. For example, in the recent years, the use of multilayered plates and shell has become very common in several industrial sectors, for example the aerospace and automotive sectors. The transverse stress and displacement components in a multilayered plate/shell are continuous functions of the thickness coordinate z; these significant particular features of layered structures were defined as C_z^0-requirement in [12, 13]: the discontinuous first derivative of the displacement field is defined as Zig-Zag effect (ZZ) and the transverse stresses continuity at the interfaces is defined as Interlaminar-Continuity (IC).

The possibility to perform an accurate analysis of a piezoelectric plate is connected with the possibility to include the so called Zig-Zag (ZZ) effect and the Interlaminar Continuity (IC). In this sense, the use of higher order plate/shell models should be preferred; an interesting observation is reported in [14] where the authors agree on the fact that at least a parabolic assumption have to be made in order to properly analyze the potential distribution along the thickness. Another example of refined theory available in literature is the model proposed in [15] by Yang and Yu.

A refined model based on the LW approach is proposed by Mitchell and Reddy in [16]: the description of the potential distribution is based on the LW approach, while the displacement field of the plate is described by means of the ESL approach. Another author who proposed an ESL model for the analysis of piezoelectric plates is Benjeddou in the work [17]. Touratier and Ossadzow-David in [18] proposed an ESL refined model able to account for the ZZ effect and the IC condition. Interested readers can be

addressed to the papers written by Saravanos and Heyliger [19] and Benjeddou [20] for a more complete discussion on electromechanical analysis of multilayered plates embedding piezo-layers.

Among all the refined theories reported in the scientific literature, the Carrera Unified Formulation (CUF) should to be mentioned. According to the CUF, the displacement field of a plate/shell is defined via an expansion of the thickness coordinate. The governing equations are derived in terms of few fundamental nuclei whose expressions do not change by varying the expansion order. In this work, the governing equations are obtained by applying the Principle of Virtual Displacement (PVD). Further details are reported in [14] and in the book [21].

In all the works and theories introduced, it is underlined that accurate analysis of plates and shells can be provided by the introduction of higher order terms, but, as a drawback, a higher computational cost is required. In the work [22] the authors investigated the possibility of obtaining refined models for plate analysis and, at the same time, of decreasing the computational cost. The axiomatic/asymptotic technique was employed: it consists in discarding all terms that do not contribute to the plate response analysis once a reference solution is defined. In [22], the authors analyzed refined models obtained according to CUF with the ESL approach and they demonstrated that the geometry (through the length-to-thickness ratio, a/h) and the ortothropic ratio (E_L/E_T ratio) influence the order and the number of the retained terms. In addition, in [23], the authors applied the axiomatic/asymptotic technique to the LW models. In addition, two different reduction criteria were proposed: the measurement of the error was conducted in different points along the thickness leading for some problems to different reduced models. Additional analyses through the axiomatic/asymptotic technique are reported in [24] where the authors employed a genetic-like algorithm in order to evaluate the Best Diagram Theory (BDT) that is a graphs which reports in function of the error the minimum number of required terms. In addition, axiomatic/asymptotic technique was employed for the analysis of refined beam theories, as reported in [25].

The present work is devoted to the analysis of refined piezoelectric plate theories through the axiomatic/asymptotic technique. In the following, the governing equations are based on a Navier-type closed form solution. The influence of several geometric and material properties is considered and two kinds of configurations are examined: sensor and actuator configurations. In the former configuration, a pressure load is applied to the top surface of the plate and the the axiomatic / asymptotic technique is applied. In the latter configuration, the potential is prescribed at the top surface of the plate and the reduced models are derived. It is intended to discover the role played by the configuration on the retained terms. An assessment with the closed form solution available in literature is conducted, i.e. with the results reported in [26].

The paper is organized as follows: a brief introduction to the piezo-mechanic equations is carried out in Section 2 and the CUF is introduced in 3. The governing equations are introduced in Section 4. The axiomatic / asymptotic technique is introduced in Section 5 and then results are reported in Section 6. Some conclusions are discussed in Section 7.

2   Preliminary

The piezoelectric effect can be explained in terms of deformations of the crystal lattice: as a mechanical (electric potential distribution) is applied to a piezoelectric material, the positions of the atoms in the crystal lattice change and this induces a potential (strain) distribution. In order to obtain the piezoelectric effect, a crystalline material must be polarized. This can be obtained by means of a potential Φ_P, which forces the microscopic polarized domains to be reordered in the same direction. According to the polarization direction, a piezoelectric material can have different coupling effects between the electric field and the mechanical deformations or stresses. The piezoelectric effect can exist if the operative temperature is below the so-called *Curie temperature*, since above this temperature the piezoelectric effect disappears due to high thermal agitation. In addition, the piezoelectric effect can disappear if the *depolarization potential* is exceeded.

In the following, multilayered piezoelectric plates are analyzed. These kind of structures are composed of N_L layers, which can be pure elastic or piezoelectric. In order to simplify the development of the mathematical model, the pure elastic layers are assumed as a particular case of piezoelectric layer, i.e. their piezoelectric coefficients are null. It is assumed, as working hypothesis, that all layers are perfectly bonded to each other. In addition, it is assumed that the physical limits of the materials are not exceeded, e.g. the Curie temperature and the depolarization potential.

The geometry and the notation of a multilayered plate is reported in Fig. 1. The reference surface is denoted as Ω and Γ is its boundary. A Cartesian reference system is employed, two main axis belong to the surface Ω (labeled as x and y) and a third axis is normal to the surface Ω. The width of this plate is denoted as a and the length is defined as b. The thickness of the plate is measured on the z axis and it is equal to h. In the following, the polarization direction of the material it is assumed parallel to the thickness direction z of the plate.

2.1 Constitutive equations

The constitutive equations for a piezoelectric layer can be written dividing the stress and deformation components into in-plane (p) and out-of-plane (n) components for a generic k layer, that is

$$\boldsymbol{\sigma}_p^k = \begin{bmatrix} \sigma_{xx}^k & \sigma_{yy}^k & \sigma_{xy}^k \end{bmatrix}^T \qquad \boldsymbol{\sigma}_n^k = \begin{bmatrix} \sigma_{xz}^k & \sigma_{yz}^k & \sigma_{zz}^k \end{bmatrix}^T$$
$$\boldsymbol{\epsilon}_p^k = \begin{bmatrix} \epsilon_{xx}^k & \epsilon_{yy}^k & \epsilon_{xy}^k \end{bmatrix}^T \qquad \boldsymbol{\epsilon}_n^k = \begin{bmatrix} \epsilon_{xz}^k & \epsilon_{yz}^k & \epsilon_{zz}^k \end{bmatrix}^T \qquad (1)$$

Direct and converse piezoelectric effects define the coupling effect between stresses and electric field. The constitutive equations are defined according to the IEEE standard [27]:

$$\boldsymbol{\sigma}_p^k = \tilde{\mathbf{C}}_{pp}^k \boldsymbol{\epsilon}_{pp}^k + \tilde{\mathbf{C}}_{pn}^k \boldsymbol{\epsilon}_{pn}^k - \mathbf{e}_p^{k^T} \mathbf{E}^k$$
$$\boldsymbol{\sigma}_n^k = \tilde{\mathbf{C}}_{pn}^{T} \boldsymbol{\epsilon}_{pp}^k + \tilde{\mathbf{C}}_{nn}^k \boldsymbol{\epsilon}_{pn}^k - \mathbf{e}_n^{k^T} \mathbf{E}^k$$
$$\boldsymbol{\mathcal{D}}^k = \mathbf{e}_p^k \boldsymbol{\epsilon}_p^k + \mathbf{e}_n^k \boldsymbol{\epsilon}_n^k + \boldsymbol{\varepsilon}^k \mathbf{E}^k \qquad (2)$$

Superscript T represents the transposition operation. $\boldsymbol{\mathcal{D}}^k$ is the electric displacement and $\mathbf{E}^k$ is the electric field:

$$\tilde{\boldsymbol{\mathcal{D}}}^k = \begin{bmatrix} \mathcal{D}_x^k & \mathcal{D}_y^k & \mathcal{D}_z^k \end{bmatrix}^T \qquad \mathbf{E}^k = \begin{bmatrix} E_x^k & E_y^k & E_z^k \end{bmatrix}^T \qquad (3)$$

The dielectric displacement is expressed in C/m^2 and the electric field is expressed in V/m. The electric field strength $\mathbf{E}^k$ can be derived from the Maxwell equations:

$$\left\{ \begin{array}{c} E_x^k \\ E_y^k \\ E_z^k \end{array} \right\} = \left\{ \begin{array}{c} -\partial_{,x} \Phi^k \\ -\partial_{,y} \Phi^k \\ -\partial_{,z} \Phi^k \end{array} \right\} \qquad (4)$$

Φ^k expresses the potential distribution for a generic k-layer. In the following, orthotropic materials are considered. The components of the matrices $\tilde{\mathbf{C}}_{pp}^k$, $\tilde{\mathbf{C}}_{pn}^k$, $\tilde{\mathbf{C}}_{np}^k$ and $\tilde{\mathbf{C}}_{nn}^k$ are the elastic material coefficients:

$$\tilde{\mathbf{C}}_{pp}^k = \begin{bmatrix} \tilde{C}_{11}^k & \tilde{C}_{12}^k & \tilde{C}_{16}^k \\ \tilde{C}_{21}^k & \tilde{C}_{22}^k & \tilde{C}_{26}^k \\ \tilde{C}_{16}^k & \tilde{C}_{26}^k & \tilde{C}_{66}^k \end{bmatrix} \quad \mathbf{C}_{pn}^k = \mathbf{C}_{np}^{k^T} = \begin{bmatrix} 0 & 0 & \tilde{C}_{13}^k \\ 0 & 0 & \tilde{C}_{23}^k \\ 0 & 0 & \tilde{C}_{33}^k \end{bmatrix} \quad \mathbf{C}_{nn}^k = \begin{bmatrix} \tilde{C}_{44}^k & \tilde{C}_{45}^k & 0 \\ \tilde{C}_{45}^k & \tilde{C}_{55}^k & 0 \\ 0 & 0 & \tilde{C}_{66}^k \end{bmatrix} \qquad (5)$$

Symbol $\tilde{}$ denotes that the material elastic coefficients are expressed in the problem reference system (i.e x, y, z system reported in Fig.1). The dependence of the elastic coefficients $\tilde{C}_{ij}$ on Young's modulus, Poisson's ratio, the shear modulus and the fiber angle is not reported. A detailed discussion is reported in the book by Reddy [10]. The in-plane and out-of-plane strain components can be computed as

$$\boldsymbol{\epsilon}_p^k = \mathbf{D}_p \mathbf{u}^k \qquad \boldsymbol{\epsilon}_n^k = \mathbf{D}_n \mathbf{u}^k \qquad (6)$$

It holds that

$$\mathbf{D}_p = \begin{bmatrix} \partial_{,x} & 0 & 0 \\ 0 & \partial_{,y} & 0 \\ \partial_{,y} & \partial_{,x} & 0 \end{bmatrix} \quad \mathbf{D}_n = \begin{bmatrix} \partial_{,z} & 0 & \partial_{,x} \\ 0 & \partial_{,z} & \partial_{,y} \\ 0 & 0 & \partial_{,z} \end{bmatrix} = \overbrace{\begin{bmatrix} 0 & 0 & \partial_{,x} \\ 0 & 0 & \partial_{,y} \\ 0 & 0 & 0 \end{bmatrix}}^{\mathbf{D}_{n\Omega}} + \overbrace{\begin{bmatrix} \partial_{,z} & 0 & 0 \\ 0 & \partial_{,z} & 0 \\ 0 & 0 & \partial_{,z} \end{bmatrix}}^{\mathbf{D}_{nz}} \qquad (7)$$

and $\mathbf{u}^k$ is the displacement vector for the generic k layer whose components are $[u_x\ u_y\ u_z]$. The operator $\partial_{,\alpha}$ denotes in a synthetic manner the derivation operator $\frac{\partial}{\partial\alpha}$ for the generic coordinate α. $\mathbf{e}_p^k$ and $\mathbf{e}_n^k$ are the matrices of the piezoelectric constants:

$$\mathbf{e}_p^k = \begin{bmatrix} 0 & 0 & 0 \\ 0 & 0 & 0 \\ e_{31}^k & e_{32}^k & e_{36}^k \end{bmatrix} \quad \mathbf{e}_n^k = \begin{bmatrix} e_{14}^k & e_{15}^k & 0 \\ e_{24}^k & e_{25}^k & 0 \\ 0 & 0 & e_{33}^k \end{bmatrix} \tag{8}$$

These constants are expressed in C/m^2. $\boldsymbol{\varepsilon}^k$ is the matrix of the permittivity coefficients of the k-layer:

$$\boldsymbol{\varepsilon}^k = \begin{bmatrix} \varepsilon_{11}^k & \varepsilon_{12}^k & 0 \\ \varepsilon_{21}^k & \varepsilon_{22}^k & 0 \\ 0 & 0 & \varepsilon_{33}^k \end{bmatrix} \tag{9}$$

In the following only hexagonal crystal systems are considered, this implies that $\varepsilon_{12} = \varepsilon_{21} = 0$ (see [27]). Permittivity constants are expressed in F/m. In the following two kind of configurations are considered: sensor and actuator configurations. Sensor configuration means that a piezoelectric plate is subjected only to external mechanical loadings and the resulting deformation state causes the potential distribution. Actuator configuration means that the deformation of a piezoelectric plate is caused by the piezoelectric layers as a consequence of the application of a potential distribution. Both configurations are synthetically reported in Fig.s 2(a) and 2(b). Further details can be found in [14] and in [21].

3   Carrera Unified Formulation

According to the Carrera Unified Formulation (CUF) the displacement field of a plate structure can be written as

$$\mathbf{u}(x,y,z) = F_\tau(z) \cdot \mathbf{u}_\tau(x,y) \qquad \tau = 1, 2, \ldots, N_{\text{EXP}} \tag{10}$$

where $\mathbf{u}$ is the displacement vector $(u_x\ u_y\ u_z)$ whose components are the displacements along the x, y, z reference axes, (see Fig. 1), F_τ is the expansion function and $\mathbf{u}_\tau = (u_{\tau x},\ u_{\tau y},\ u_{\tau z})$ are the displacement variables. N_{EXP} is the number of terms of the expansion. The implementation of the CUF can be based on two schemes: the Equivalent Single Layer (ESL) or Layer Wise (LW). In the following both schemes are discussed.

3.1   Equivalent Single Layer

According to the ESL approach, a multilayered heterogeneous plate is analyzed as a single equivalent lamina. In this case F_τ functions can be considered as Taylor expansions of z, that is $F_\tau = z^{\tau-1}$. The number of unknowns is not dependent on the number of the plate layers. Examples of linear and higher order displacement fields are reported in Fig. 3(a). The position of a point P on the thickness is indicated with z_P. In the following, the ESL models are synthetically indicated as EN, where N is the expansion order. An example of an E4 displacement field is reported

$$\begin{aligned} u_x &= u_{x_1} + z\, u_{x_2} + z^2\, u_{x_3} + z^3\, u_{x_4} + z^4\, u_{x_5} \\ u_y &= u_{y_1} + z\, u_{y_2} + z^2\, u_{y_3} + z^3\, u_{y_4} + z^4\, u_{y_5} \\ u_z &= u_{z_1} + z\, u_{z_2} + z^2\, u_{z_3} + z^3\, u_{z_4} + z^4\, u_{z_5} \end{aligned} \tag{11}$$

As mentioned in [22], classical models such as CLT and FSDT can be considered special cases of full linear expansion (E1).

3.2   Layer Wise Theories

According to the Layer Wise scheme, the displacement field is defined as a continuous function along the thickness direction and it is defined independently in each layer. The displacement continuity is imposed at the layers interfaces. In this case the theories can be conveniently built by using Legendre's polynomials expansion. An example of linear and higher order LW displacement field is reported in Fig. 3(b), the position of a point P on the thickness is defined according to a layer local reference system x_k,

y_k, and ζ_k. The main axes of the local reference system are parallel to the x, y, z reference system, but its origin with respect to the z axis is located at the middle of the layer k. The displacement field is described as

$$\mathbf{u}^k = F_t \cdot \mathbf{u}_t^k + F_b \cdot \mathbf{u}_b^k + F_r \cdot \mathbf{u}_r^k = F_\tau \mathbf{u}_\tau^k \qquad \tau = t, b, r \;\; r = 2, 3, \dots, N \qquad k = 1, 2, \dots, N_L \qquad (12)$$

Subscripts t and b correspond to the top and the bottom of a layer. Functions F_τ depend on a coordinate ζ_k and its range is $-1 \le \zeta_k \le 1$. The extremal values -1 and 1 are reached at the bottom and at the top of the layer. Functions F_τ derive from the Legendre's polynomials P according to the following equations.

$$F_t = \frac{P_0 + P_1}{2} \qquad F_b = \frac{P_0 - P_1}{2} \qquad F_r = P_r - P_{r-2} \qquad r = 2, 3, \dots, N \qquad (13)$$

The Legendre's polynomials used for fourth-order theory are:

$$P_0 = 1 \quad P_1 = \zeta_k \quad P_2 = \frac{3\zeta_k^2 - 1}{2} \quad P_3 = \frac{5\zeta_k^3 - 3\zeta_k}{2} \quad P_4 = \frac{35\zeta_k^4}{8} - \frac{15\zeta_k^2}{4} + \frac{3}{8} \qquad (14)$$

The LW models ensure the compatibility of the displacement between layers, that is, the 'zig-zag' effects by definition:

$$\mathbf{u}_t^k = \mathbf{u}_b^{k+1} \qquad k = 1, \dots, N_l - 1 \qquad (15)$$

In the following, the LW models are denoted by the acronym LN, N is the expansion order. An example of L4 layer displacement field is

$$
\begin{aligned}
u_x^k &= F_t u_{xt}^k + F_2 u_{x2}^k + F_3 u_{x3}^k + F_4 u_{x4}^k + F_b u_{xb}^k \\
u_y^k &= F_t u_{yt}^k + F_2 u_{y2}^k + F_3 u_{y3}^k + F_4 u_{y4}^k + F_b u_{yb}^k \\
u_z^k &= F_t u_{zt}^k + F_2 u_{z2}^k + F_3 u_{z3}^k + F_4 u_{z4}^k + F_b u_{zb}^k
\end{aligned}
\qquad (16)
$$

More details about CUF can be found in [21], [28] and [29].

3.3 Potential distribution assumption

The layers of the the multilayered plates herein considered can be piezoelectric or pure elastic. In this case, the differences of the electric properties of each layer can be significant. In the following the electric potential distribution is expressed according to a LW form distribution since an ESL scheme seems to not be appropriate in order to cover high gradients. The potential distribution is then defined as:

$$\Phi = F_t \Phi_t + F_r \Phi_r + F_b \Phi_b = F_\tau \Phi_\tau \qquad \tau = t, r, b \;\; r = 2, 3, 4 \qquad (17)$$

The continuity of the potential distribution at the layers interfaces has to be imposed:

$$\Phi_t^k = \Phi_b^{k+1} \qquad k = 1, \cdots, N_L - 1 \qquad (18)$$

The expansion order of the potential distribution is assumed to be equal to the expansion order of the displacement field, independently from the adopted scheme (ESL or LW). The potential distribution is a scalar quantity, but for implementation reasons it is convenient to define it as a vector, i.e. $\mathbf{\Phi}^k = \left[\Phi^k \; \Phi^k \; \Phi^k\right]^T$. In this case the electric field strength can be expressed as

$$\mathbf{E}^k = \mathbf{D}_e \mathbf{\Phi}^k \qquad (19)$$

where

$$\mathbf{D}_e = \begin{bmatrix} -\partial_{,x} & 0 & 0 \\ 0 & -\partial_{,y} & 0 \\ 0 & 0 & -\partial_{,z} \end{bmatrix} = \underbrace{\begin{bmatrix} -\partial_{,x} & 0 & 0 \\ 0 & -\partial_{,y} & 0 \\ 0 & 0 & 0 \end{bmatrix}}_{\mathbf{D}_{e\Omega}} + \underbrace{\begin{bmatrix} 0 & 0 & 0 \\ 0 & 0 & 0 \\ 0 & 0 & -\partial_{,z} \end{bmatrix}}_{\mathbf{D}_{ez}} \qquad (20)$$

4 Governing equation and Navier-type solution

The analysis of a plate can be conducted by means of the Principle of Virtual Displacement (PVD) which states that:

$$\delta L_{int} = \delta L_{ext} \tag{21}$$

where δL_{ext} is the virtual variation of the external loadings work and δL_{int} is the virtual variation of the internal strain energy. Considering the in-plane (p) and out-of-plane (n) components of the stresses and strains, it is possible to write:

$$\int_V \left(\delta\boldsymbol{\epsilon}_p^T \cdot \boldsymbol{\sigma}_p + \delta\boldsymbol{\epsilon}_n^T \cdot \boldsymbol{\sigma}_n - \delta\mathbf{E}^T \, \boldsymbol{\mathcal{D}} \right) dV = \delta\, L_e \tag{22}$$

δ denotes the virtual variation. The development of this equation is herein omitted for the sake of brevity. Details can be found in [14] and in the book [21]. The static response can be evaluated solving the equation:

$$\sum_{k=1}^{N_l} \int_{\Omega_k} \left\{ (\mathbf{D}_p \delta\mathbf{u}_\tau^\tau)^T F_\tau \left[\left(\tilde{\mathbf{C}}_{pp}^k \mathbf{D}_p + \tilde{\mathbf{C}}_{pn}^k \mathbf{D}_n \right) F_s \mathbf{u}_s^k - \mathbf{e}_p^k \mathbf{D}_e F_s \Phi_s^k \right] + \right.$$

$$+ \left(\mathbf{D}_n \delta\mathbf{u}_\tau^k \right)^T F_\tau \left[\left(\tilde{\mathbf{C}}_{np}^k \mathbf{D}_p + \tilde{\mathbf{C}}_{nn} D_n \right) F_s \mathbf{u}_s^k - \mathbf{e}_n^{k^T} \mathbf{D}_e F_s \Phi_s^k \right] -$$

$$\left. - \left(\mathbf{D}_e \delta\Phi_\tau^k \right)^T F_\tau \left[\left(\mathbf{e}_p^k \mathbf{D}_p + \mathbf{e}_n^k \mathbf{D}_n \right) F_s \mathbf{u}_s^k + \boldsymbol{\varepsilon}^k \mathbf{D}_e F_s \Phi^k \right] \right\} dV = \sum_{k=1}^{N_L} \delta\, L_{ext}^k \tag{23}$$

δL_{ext}^k is the virtual variation of the external loadings for the generic k-layer and N_L is the total number of layers. This equation can be solved applying the integration by parts

$$\int_\Omega \left(\mathbf{D}_\chi \delta\mathbf{u}^T \right)^T \mathbf{u}^k d\Omega_k = -\int_\Omega \delta\mathbf{u}^{k^T} \mathbf{D}_\chi^T \mathbf{u}^k \, d\Omega + \int_\Gamma \delta\mathbf{u}^{k^T} \mathbf{I}_\chi \mathbf{u}^k \, d\Gamma_k \tag{24}$$

where $\chi = (p,\ n\Omega,\ e\Omega)$ and

$$\mathbf{I}_p = \begin{bmatrix} 1 & 0 & 0 \\ 0 & 1 & 0 \\ 1 & 1 & 0 \end{bmatrix} \qquad \mathbf{I}_{n\Omega} = \begin{bmatrix} 0 & 0 & 1 \\ 0 & 0 & 1 \\ 0 & 0 & 0 \end{bmatrix} \qquad \mathbf{I}_{e\Omega} = \begin{bmatrix} -1 & 0 & 0 \\ 0 & -1 & 0 \\ 0 & 0 & 0 \end{bmatrix} \tag{25}$$

All the passages are not reported for the sake of brevity. The final result is:

$$\sum_{k=1}^{N_L} \int_{\Omega_k} \int_{A_k} \left\{ \delta\mathbf{u}_s^{k^T} \left[-\mathbf{D}_p^T F_s \left(\tilde{\mathbf{C}}_{pp}^k \mathbf{D}_p F_\tau \mathbf{u}_\tau^k + \tilde{\mathbf{C}}_{pn}^k \left(\mathbf{D}_{n\Omega} + \mathbf{D}_{nz} \right) F_\tau \mathbf{u}_\tau^k - \mathbf{e}_p^{k^T} \left(\mathbf{D}_{e\Omega} + \mathbf{D}_{ez} \right) F_\tau \Phi_\tau^k \right) + \right.\right.$$

$$+ \left(\mathbf{D}_{nz}^T - \mathbf{D}_{n\Omega}^T \right) F_s \left(\tilde{\mathbf{C}}_{np}^k \mathbf{D}_p F_\tau \mathbf{u}_\tau^k + \tilde{\mathbf{C}}_{nn}^k \left(\mathbf{D}_{n\Omega} + \mathbf{D}_{nz} \right) F_\tau \mathbf{u}_\tau^k - \mathbf{e}_n^{k^T} \left(\mathbf{D}_{e\Omega} + \mathbf{D}_{ez} \right) F_\tau \Phi_\tau^k \right) +$$

$$\left. +\delta\Phi_s^{k^T} \left[\left(\mathbf{D}_{ez}^T - \mathbf{D}_{e\Omega}^T \right) F_\tau \left(\mathbf{e}_p^k \mathbf{D}_p + \mathbf{e}_n^k \left(\mathbf{D}_{n\Omega} + \mathbf{D}_{nz} \right) F_\tau \mathbf{u}_\tau^k + \boldsymbol{\varepsilon}^k \left(\mathbf{D}_{e\Omega} + \mathbf{D}_{ez} \right) F_\tau \Phi_\tau^k \right) \right] \right\} dz\, d\Omega_k +$$

$$+\sum_{k=1}^{N_L} \int_{\Gamma_k} \int_{A_k} \left\{ \delta\mathbf{u}_s^{k^T} \left[\mathbf{I}_p^T F_\tau \left(\tilde{\mathbf{C}}_{pp}^k \mathbf{D}_p F_\tau \mathbf{u}_\tau^k + \tilde{\mathbf{C}}_{pn}^k \left(\mathbf{D}_{n\Omega} + \mathbf{D}_{nz} \right) F_\tau \mathbf{u}_\tau^k - \mathbf{e}_p^{k^T} \left(\mathbf{D}_{e\Omega} + \mathbf{D}_{ez} \right) F_\tau \Phi_\tau^k \right) + \right.\right.$$

$$+ \mathbf{I}_{n\Omega}^T F_s \left(\tilde{\mathbf{C}}_{np}^k \mathbf{D}_p F_\tau \mathbf{u}_\tau^k + \tilde{\mathbf{C}}_{nn}^k \left(\mathbf{D}_{n\Omega} + \mathbf{D}_{nz} \right) F_\tau \mathbf{u}_\tau^k - \mathbf{e}_n^{k^T} \left(\mathbf{D}_{e\Omega} + \mathbf{D}_{ez} \right) F_\tau \Phi_\tau^k \right) +$$

$$\left.\left. +\delta\Phi_\tau^{k^T} \left[\mathbf{I}_{e\Omega}^T F_\tau \left(\mathbf{e}_p^k \mathbf{D}_p + \mathbf{e}_n^k \left(\mathbf{D}_{n\Omega} + \mathbf{D}_{nz} \right) F_\tau \mathbf{u}_\tau^k + \boldsymbol{\varepsilon}^k \left(\mathbf{D}_{e\Omega} + \mathbf{D}_{ez} \right) F_\tau \Phi_\tau^k \right) \right] \right\} dz\, d\Gamma_k = \sum_{k=1}^{N_L} \delta L_{ext}^k \right.$$

$$\tag{26}$$

The operator $\int_{A_k} dz$ denotes the integration in the thickness direction for a generic k-layer. Further details can be found in [14]. In the book [21] further informations can be found, in particular for the

application of the Reissner mixed variational theorem to the analysis of piezoelectric plates. The attention has been here restricted to the case of closed form solutions related to simply supported, cross-ply orthotropic rectangular plates ($\tilde{C}_{16} = \tilde{C}_{26} = \tilde{C}_{36} = \tilde{C}_{45} = 0$) loaded by a transverse distribution of harmonic loadings. The displacement and potential functions are therefore express in the following harmonic form:

$$
\begin{aligned}
u_{x_\tau}^k &= \hat{U}_{x_\tau}^k \cdot \cos\left(\frac{m\pi x_k}{a_k}\right) \sin\left(\frac{n\pi y_k}{b_k}\right) & k &= 1, N_L \\
u_{y_\tau}^k &= \hat{U}_{y_\tau}^k \cdot \sin\left(\frac{m\pi x_k}{a_k}\right) \cos\left(\frac{n\pi y_k}{b_k}\right) & \tau &= 1, N_{\text{EXP}} \\
u_{z_\tau}^k &= \hat{U}_{z_\tau}^k \cdot \sin\left(\frac{m\pi x_k}{a_k}\right) \sin\left(\frac{n\pi y_k}{b_k}\right) & & \\
\Phi_\tau^k &= \hat{\Phi}_\tau^k \cdot \sin\left(\frac{m\pi x_k}{a_k}\right) \sin\left(\frac{n\pi y_k}{b_k}\right) & &
\end{aligned}
\tag{27}
$$

where $\hat{U}_{x_\tau}^k$, $\hat{U}_{y_\tau}^k$, $\hat{U}_{z_\tau}^k$ and $\hat{\Phi}_\tau^k$ are the amplitudes, m and n are the number of half-waves (the range varies from 0 to ∞) and a_k and b_k are the dimensions of the plate. The same solution can be applied to ESL approach, in this case, the displacement variables appear without the superscript k.

5 Reduced refined models construction

A refinement of the results of plate and shell models can be obtained by means of the introduction of high order terms but the price to pay is a higher computational cost. A possibility to reduce it, is offered by the axiomatic / asymptotic technique which aims to evaluate the effectiveness of each term. This technique was proposed in [22] and it consists in the following steps:

1. plate parameters such as the geometry, boundary conditions (BCs), loadings, materials and layer layouts, are fixed;

2. a set of output parameters is chosen, such as displacement and stress components;

3. a theory is fixed, that is the displacement variables to be analyzed are defined;

4. a reference solution is defined; in the present work L4 approach is adopted, since this fourth-order model offers an excellent agreement with the three-dimensional solutions as highlighted in [22] and in [23];

5. CUF is used to generate the governing equations for the theories considered;

6. each single term of the refined model is deactivated and the error is than measured. If the error exceed a defined threshold the term under exam is considered as essential. In the following the threshold is set equal to 0.05%.

There are several ways to compute the error, in the present work the error is calculated as follows:

$$
e = 100 \cdot \left| 1 - \frac{Q}{Q_{\text{ref}}} \right|
\tag{28}
$$

where Q is the quantity under exam (as the stress component σ_{xx} or a displacement component u_x) and Q_{ref} is the reference value. The points at which the error is computed depend on the quantity analyzed. In previous works, as [22] and [23], several criteria were proposed. In this work, the error is computed at $[a/2, b/2, h/2]$ for u_z, σ_{xx} and σ_{zz}, at $[a/2, 0, 0]$ for σ_{xz} and ϕ, at $[0, b/2, 0]$ for σ_{yz} if the sensor configuration is considered. Instead if the actuator configuration is considered, the stress σ_{zz} is evaluated at $[a/2, b/2, 0]$ since its value at the top and bottom surfaces is zero and a small error at these points can lead to overestimate the number of required terms. This criterium is defined as C1. In the following, the results are represented in a synthetic manner, the legend is reported in Table 1. An example of representation of a reduced model is reported in the following. Let's consider a two layer piezoelectric plate and its relative L4 model:

$$u_x = F_t\, u^1_{xt} + F_2\, u^1_{x2} + F_3\, u^1_{x3} + F_4\, u^1_{x4} + F_b\, u^1_{xb} + F_t\, u^2_{xt} + F_2\, u^2_{x2} + F_3\, u^2_{x3} + F_4\, u^2_{x4} + F_b\, u^2_{xb}$$
$$u_y = F_t\, u^1_{yt} + F_2\, u^1_{y2} + F_3\, u^1_{y3} + F_4\, u^1_{y4} + F_b\, u^1_{yb} + F_t\, u^2_{yt} + F_2\, u^2_{y2} + F_3\, u^2_{y3} + F_4\, u^2_{y4} + F_b\, u^2_{yb}$$
$$u_z = F_t\, u^1_{zt} + F_2\, u^1_{z2} + F_3\, u^1_{z3} + F_4\, u^1_{z4} + F_b\, u^1_{zb} + F_t\, u^2_{zt} + F_2\, u^2_{z2} + F_3\, u^2_{z3} + F_4\, u^2_{z4} + F_b\, u^2_{zb}$$
$$\Phi = F_t\, \Phi^1_t + F_2\, \Phi^1_2 + F_3\, \Phi^1_3 + F_4\, \Phi^1_4 + F_b\, \Phi^1_b + F_t\, \Phi^2_t + F_2\, \Phi^2_2 + F_3\, \Phi^2_3 + F_4\, \Phi^2_4 + F_b\, \Phi^2_b \tag{29}$$

The full model can be represented as reported in Table 2 and it is labeled as "Full model". If terms u^1_{x2}, u^1_{y4}, u^1_{z3}, u^2_{x2}, Φ^1_1, Φ^2_1 are discarded, the reduced model becomes:

$$u_x = F_t\, u^1_{xt} + F_2\, u^1_{x2} + F_3\, u^1_{x3} + F_4\, u^1_{x4} + F_b\, u^1_{xb} + F_t\, u^2_{xt} + \qquad\quad + F_3\, u^2_{x3} + F_4\, u^2_{x4} + F_b\, u^2_{xb}$$
$$u_y = F_t\, u^1_{yt} + F_2\, u^1_{y2} + F_3\, u^1_{y3} + \qquad\quad + F_b\, u^1_{yb} + F_t\, u^2_{yt} + F_2\, u^2_{y2} + F_3\, u^2_{y3} + F_4\, u^2_{y4} + F_b\, u^2_{yb}$$
$$u_z = F_t\, u^1_{zt} + F_2\, u^1_{z2} + \qquad\quad + F_4\, u^1_{z4} + F_b\, u^1_{zb} + F_t\, u^2_{zt} + F_2\, u^2_{z2} + F_3\, u^2_{z3} + F_4\, u^2_{z4} + F_b\, u^2_{zb}$$
$$\Phi = F_t\, \Phi^1_t + \qquad\quad + F_3\, \Phi^1_3 + F_4\, \Phi^1_4 + F_b\, \Phi^1_b + F_t\, \Phi^2_t + \qquad\quad + F_3\, \Phi^2_3 + F_4\, \Phi^2_4 + F_b\, \Phi^2_b \tag{30}$$

and it is represented as reported in Table 2 and it is labeled as "Reduced model". Attention has to be paid during the deactivation process: the terms related with the functions F_t and F_b for both mechanical displacement variables (when LW approach is employed) and electric displacement variables cannot be suppressed since in these cases the continuity condition on displacement and electric variables ($\mathbf{u}^k_t = \mathbf{u}^{k+1}_b$, $\Phi^k_t = \Phi^{k+1}_b$) is imposed.

6 Comments on results

In the following, reduced models for simply supported piezoelectric plates are reported. As already introduced, two different configurations are considered: sensor and actuator configurations. When a sensor configuration is considered, a transverse pressure is applied to the top surface of the plate and a potential distribution is generated. The potential at the top and at the bottom is set to zero. When an actuator configuration is considered the deformation state of a plate is originated by the imposition of a potential distribution: the value of the potential is set to 1 V at the top and to 0 V at the bottom of the plate. In the following, the sensor and actuator configurations will be defined as problem 1 and problem 2 respectively and they are:

$$p_z = \hat{p}_0\, \sin\left(\frac{m\,\pi}{a}\, x\right) \sin\left(\frac{n\,\pi}{b}\, y\right) \qquad \text{Sensor configuration} \tag{31}$$

$$\Phi = \hat{\Phi}_0\, \sin\left(\frac{m\,\pi}{a}\, x\right) \sin\left(\frac{n\,\pi}{b}\, y\right) \qquad \text{Actuator configuration} \tag{32}$$

where $m = n = 1$. The reference system layout and the representation of the two configurations are reported in Fig.s 1, 2(a) and 2(b), respectively.

6.1 Model assessment

The axiomatic/asymptotic analysis requires a reference solution in order to evaluate the effectiveness of the terms in the model. An exact analytical solution would be the best option. Anyway, these solutions are available for only few problems and, in some cases, the values are referred to only few points. In the previous works on axiomatic/asymptotic analysis, the L4 proved to offer solutions in agreement with the exact solutions available in the scientific literature. Herein, an assessment of the L4 model is carried out for the piezoelectric case with respect the case analyzed in [26]. The L4 model assessment considers a four layers laminated plate: the two piezoelectric layers are located at the top and the bottom. The elastic materials properties are: $E_1 = 132.38 \times 10^9$ Pa, $E_2 = E_3 = 10.756 \times 10^9$ Pa, $G_{12} = G_{13} = 5.6537 \times 10^9$ Pa, $G_{23} = 3.606 \times 10^9$ Pa, $\nu_{12} = \nu_{13} = 0.24$, $\nu_{23} = 0.49$, $\epsilon_{11} = 3.098966 \times 10^{-11}$ F/m, $\varepsilon_{22} = \varepsilon_{33} = 2.6562563 \times 10^{-11}$ F/m. The total thickness of these layers is equal to $h = 0.8 \cdot h_{\text{TOT}}$ and the ply sequence is $90°/0°$. The piezoelectric layers are made of PZT-4 and its properties are: $E_1 = E_2 = 81.3 \times 10^9$ Pa, $E_3 = 64.5 \times 10^9$ Pa, $\nu_{12} = 0.329$, $\nu_{13} = \nu_{23} = 0.432$, $G_{44} = G_{55} = 25.6 \times 10^9$,

$G_{66} = 30.6 \times 10^9$, $e_{31} = e_{32} = -5.20$ C/m^2, $e_{33} = 15.08$ C/m^2, $e_{24} = e_{15} = 12.72$ C/m^2, $\varepsilon_{11}/\varepsilon_0 = \varepsilon_{22}/\varepsilon_0 = 1475$, $\varepsilon_{33}/\varepsilon_0 : 1300$. ε_0 is the vacuum permittivity, which is equal to 8.854187×10^{-12} F/m. The thickness is $h = 0.1 \cdot h_{\text{TOT}}$ per each piezoelectric layer. The results are reported in Table 3 and in Table 4 for sensor and actuator configurations. It is possible to note that the L4 model offers a good agreement with the exact solution and for this reason it is used as reference solution for the axiomatic / asymptotic analysis.

6.2 Isotropic core plate

An isotropic plate with two piezoelectric layers at the top and at the bottom is considered. The isotropic material is titanium. Its properties are: $E = 114$ GPa, $\nu = 0.3$ and $\varepsilon_{11,22,33} = 8.85 \times 10^{-12}$ F/m and the thickness is $h_{core} = 0.8\,h_{\text{TOT}}$. The two piezoelectric layers are made of PZT-4 and their thickness is $h_{piezo} = 0.1\,h_{\text{TOT}}$. The properties of this material were already described for the assessment of L4 model. In the following E4 and L4 refined models are analyzed.

The most significant values employed in the analysis of the relevance of terms are reported in Tables 5 and 6 for problems 1 and 2, respectively. For the sake of brevity not all values of all quantities involved in the axiomatic/asymptotic technique are reported.

Results of the axiomatic/asymptotic analysis are reported in Table 7 for both problems 1 and 2 considering the E4 model. The results are related only to the reduced models for displacement u_z (problem 1) and to potential Φ (problem 2), since for all the other stress or displacement components all displacement variables are relevant. As first observation, it is possible to state that thick plates analysis is more critical than thin plates analysis since more terms are required. Moreover, it stands out that the difference between the reduced models for problem 1 and 2 is particular clear when a thin plate is considered: the reduced model for problem 2 has only the terms related with Φ_t^k and Φ_b^k. It is possible to state that for this particular problem the potential distribution tends to be quasi uncoupled from the mechanical analysis.

The distribution of the potential Φ and the displacement u_z for the thin plate case are evaluated by means of the reduced models reported in Table 7 (sensor and actuator configuration respectively) and in Fig.s 4(a) and 5(a) their distributions are reported. It is possible to note the good agreement offered by the reduced models at the reference point with the reference solution.

Reduced L4 models are reported in Tables 8 and 9 for problems 1 and 2 respectively. As first remark, it is possible to note that in general for both problems the models for thick plate analysis require more displacement variables than for thin plate analysis. It is interesting to observe that the fourth-order terms are rarely included in the refined models reported for the problem 1 (Table 8). In particular, these higher-order terms are totally excluded when a thin plate is considered. In addition the models reported in table 8 highlight that in almost all cases the potential distribution can be described by means of a linear model (i.e. considering only Φ_t^k and Φ_b^k functions). Considering the reduced models for problem 2 (Table 9) and for problem 1 (Table 8), it is interesting to note that the type of configuration influences the number and the order of the terms selected. For example, in the reduced model for the displacement u_z the variables u_{x1}^1, u_{y1}^1 and u_{z1}^1 are included when problem 2 is considered but the same are not included when a problem 1 is considered. In general, the reduced models for the problem 1 require less displacement variables than for problem 2. As already noted for the problem 1, the fourth-order terms are rarely included for problem 2, but in most of cases the potential distribution computation requires more displacement variables than only Φ_t^k and Φ_b^k, although the reduced model for potential Φ requires only the top and bottom functions (F_t^k, F_b^k, Φ_t^k and Φ_b^k).

The distribution of stress σ_{zz} and displacement u_z along the thickness direction are reported in Fig.s 6 and 7 for L4 reduced model. Problems 1 and 2 are considered, respectively. It is possible to note that for both problems the reduced models offer values whose accuracies are within the a-priori defined threshold at the considered error criterium points. Anyway, a deviation from the reference solution can be noted for the stress σ_{zz} when the attention is restricted to the thick plates for problem 1 (Fig. 6) or when problem 2 is considered (Fig. 7). It can be observed that the accuracy in the stress computation depends on the type of configuration, indeed the stress distribution is more accurately computed for problem 2 than problem 1.

6.3 Laminated core plates

Axiomatic/asymptotic analysis is herein conducted considering a laminate plate. Its properties and geometry have been already introduced when the assessment of L4 model for the piezo-mechanic analysis has been performed. The reference values of all quantities are not reported for the sake of brevity in Tables 10 and 11. Only few values for displacement u_z, potential Φ and stress σ_{zz} are reported for both problems 1 and 2, respectively.

The E4 model is analyzed and the results are presented in Table 12; it is possible to observe that, as already noted for the metallic plate, the type of configuration adopted influences the displacement/stress components which take advantage of term reduction technique. In addition, it is possible to note that thick plate analysis is more critical than thin plate analysis, since more displacement variables are required. It is interesting to note that the potential distribution for a thin laminate plate in actuator configuration (problem 2) can be computed with an acceptable accuracy by means of a linear model (only Φ_t^k and Φ_b^k are involved). It is possible to state that, similarly to the isotropic core case, the potential distribution tends to be quasi uncoupled.

The displacement u_z and potential Φ distribution with the thickness direction are reported in Fig. 4(b) and 5(b). The reduced models proposed in Table 12 are employed. In both cases, it is possible to note the good agreement of the solution offered by the reduced models with the reference solution.

In the following, L4 models is analyzed. The reduced L4 models for problem 1 and 2 are reported in Tables 13 and 14, respectively. Firstly, it can be noted that when problem 1 is considered (Table 13) the analysis of a thick plate requires more displacement variables than the analysis of a thin plate. In addition, the reduced combined model for a thick plate has more than the 50% of the terms while the same model for a thin plate has less than the 50% of the displacement variables. It is possible to note that the two types of configurations lead to different reduced models: differences exist in terms of number and order of the retained terms. As an example, it is possible to note the relevance of terms u_{x1}^1, u_{y1}^1 and u_{y1}^1 (i.e. the terms u_{x1}, u_{y1} and u_{y1} related with the first layer) in the case of the reduced model for the displacement u_z, in thick plate case. It should be underlined that, as already reported for the isotropic core plate, the potential distribution Φ, when problem 2 is considered, has only the terms related with the top and bottom functions (F_t^k and F_b^k, see Table 14). This observation holds for thick and thin geometries. It is worth noting that the fourth-order terms are rarely included in all problems, as already underlined for the isotropic core plate.

The distributions of the stress σ_{zz} and potential Φ along the thickness direction computed by means of the reduced combined models of Table 13 are reported in Fig. 8. It is possible to observe the good agreement with the reference solution. In addition, the distribution of the stress σ_{zz} and displacement u_z with the thickness direction are reported in Fig. 9. In this case, the reduced combined models employed to compute these quantities are in Table 14. It can be noted that the values are correctly computed (i.e. the accuracy is within the a-priori threshold) at the error criterium points although, in some case, the distribution may differ from the reference solution.

7 Conclusions

Simply supported piezoelectric plates have been analyzed. Navier-type solution has been adopted and the Carrera Unified Formulation has been employed to generate the refined models. The axiomatic / asymptotic technique has been used to detect the terms which are essential for a proper static response analysis. The effectiveness of the terms of a model has been computed by deactivating all terms one-by-one and by comparing the response with respect to a reference solution. If the error committed is below a defined threshold, the term is considered as not relevant and then discarded. In the present work, the reference solution has been obtained by means of L4 model, since it has been demostrated that this model gives the best agreement with the exact solutions available in literature for piezoelectric analysis. The influence of the geometry has been considered through the length-to-thickness (a/h) ratio and both sensor and actuator configurations were analyzed. The results have shown that

1. thick plate analysis is more crtical than thin plate analysis, since more terms are required. This is valid for both types of configurations;

2. the relevance of the terms is influenced by the type of the configuration considered, in other words reduced models for problem 1 are different from the reduced models for problem 2;

3. the description of the potential distribution in the thickness direction for a thin isotropic and laminated plate can be performed considering a quasi decoupled model, that is, only Φ_t and Φ_b can be retained;

In addition, the CUF theory has proved to be a versatile means to analyze piezoelectric plates and to deal with a method that could be defined as a mixed axiomatic/asymptotic. In particulars the CUF makes it possible:

1. to analyze the accuracy of each problem variable by comparing the results with full refined models;

2. to consider the accuracy of the results as an input, and to detect the minimum set of variables required to fulfill the accuracy input.

Future works can be performed considering different BC (in this case the use of FEM is mandatory) and a genetic approach can be used to obtain a Best Plate Diagram Theory which reports the number of retained terms vs the committed error for different refined models and geometries. In addition, shell geometries can be considered and the effect of a piezo-thermal load on the retained displacement variables can be analyzed.

References

[1] Curie, J. and Curie, P. D'eveloppement par compression de l'électricité polaire dans les cristaux hémiédres a faces inclinées. C. R. Acad. Sci. Paris, 91:294–295, 1880.

[2] Cady, W.G. *Piezoelectricity*. Dover, 1964.

[3] Tiersten, H.F. *Linear Piezoelectric Plate Vibrations*. Plenum Press, 1969.

[4] Ikeda, T. *Fundamentals of Piezoelectricity*. Oxford University Press, 1996.

[5] Ahmad, I. Smart structures and materials. in proceedings of us army research office workshop on smart materials, structures and mathematical issues. 1988.

[6] Rogers, C.A. Intelligent material systems and structures. In *In Proceedings of US Japan Workshop on Smart/Intelligent Materials and Systems*, 1990.

[7] Sirohi, J. and Chopra, I. Fundamental understanding of piezoelectric strain sensors. *J. Intell. Mater. Syst. Struct.*, 11:246–257, 2000.

[8] Chopra, I. Status of application of smart structures technology to rotorcraft systems. *J. Am. Helicopter Soc.*, 45:228–252, 2000.

[9] Gaudenzi, P. *Smart Structures: Physical Behaviour, Mathematical Modelling and Applications*. John Wiley & Sons, Ltd, UK, 2009.

[10] Reddy, J. N. *Mechanics of Laminated Plates, Theory and Analysis*. CRC Press, Boca Raton, 1997.

[11] Mindlin, R. High frequency vibrations of piezoelectric crystal plates. *Int J Solids Struct.*, 8:895–906, 1972.

[12] Carrera, E. A class of two dimensional theories for multilayered plates analisys. *Atti Acc. Sci. Torino*, 19-20:49–87, 1995.

[13] Carrera, E. C_z^0 requirements - models for the two dimensional analysis of multilayered structures. *Composite Structures*, 37(3-4):373–383, 1997.

[14] Ballhause, D. and D'Ottavio, M. and Kroplin, B. and Carrera, E. A unified formulation to assess multilayered theories for piezoelectric plates. *Computer & Structures*, 83:1217–1235, 2005.

[15] Yang, J. and Yu, J. Equations for a laminated piezoelectric plate. *Arch. Mech.*, 45:653–664, 1993.

[16] Mitchell, J. and Reddy, J. N. A refined hybrid plate theory for composite laminates with piezoelectric laminae. *Int. J. Solids Structures*, 32(16):2345–67, 1995.

[17] Benjeddou, A. and Deu, J. F. A two-dimensional closed-form solution for the free-vibrations analysis of piezoelectric sandwich plates. *Int. J. Solids Structures*, 39:1463–86, 2001.

[18] Touratier, M. and Ossadzow-David, C. Multilayered piezoelectric refined plate theory. *AIAA*, 41(1):90–9, 2003.

[19] Saravanos, D. and Heyliger, P. Mechanics and computational models for laminated piezoelectric beams, plates and shells. *Appl Mech Rev*, 52(10):305–320, 1999.

[20] Benjeddou, A. Advances in piezoelectric finite element modeling of adaptive structural elements: a survey. *Computer & Structures*, 76(1-3):347–63, 2000.

[21] Carrera, E. and Brischetto, S. and Nali, P. *Plates and Shells for Smart Structures Classical and Advanced Theories for Modeling and Analysis*. Wiley, New Delhi, 2011.

[22] Carrera, E. and Petrolo, M. Guidelines and recommendation to construct theories for metallic and composite plates. *AIAA Journal*, 48(12):2852–2866, 2010.

[23] Petrolo, M. and Lamberti, A. Axiomatic/asymptotic analysis of refined layer-wise theories for composite and sandwich plates. *Mechanics of Advanced Materials and Structures*, 2013. In press.

[24] Carrera, E. and Miglioretti, F. Selection of appropriate multilayered plate theories by using a genetic like algorithm. *Composite Structures*, 94(3):1175 – 1186, 2012.

[25] Carrera, E. and Petrolo, M. On the effectiveness of higher-order terms in refined beam theories. *Journal of Applied Mechanics*, 78:1–17, 2011.

[26] Heyliger, P. Static behavior of laminated elastic/piezoelectric plates. *AIAA Journal*, 32(12):2481 – 2484, 1994.

[27] A.N.S. Institute. Ieee standard on piezoelectricity. Technical Report NASA CR 4665, IEEE, March 1987.

[28] Carrera, E. Theories and finite elements for multilayered plates and shells: A unified compact formulation with numerical assessment and benchmarking. *Arch. Comput. Meth. Engng*, 10(3):215–296, 2003.

[29] Carrera, E. and Giunta, G., and Petrolo, M. *Beam Structures, Classical and Advanced Theories*. Wiley, New Delhi, 2011.

[30] Pagano, J. N. Exact solutions for rectangular bidirectional composites and sandwich plate. *Journal of Composites Material*, 4:20–34, 1969.

Tables

Active term	Inactive term	Non-deactivable term
▲	△	■

Table 1: Symbols to indicate the status of a displacement variable.

	Full model										Reduced model							
■	▲	▲	▲	■	▲	▲	▲	■		■	▲	▲	▲	■	△	▲	▲	■
■	▲	▲	▲	■	▲	▲	▲	■		■	▲	▲	△	■	▲	▲	▲	■
■	▲	▲	▲	■	▲	▲	▲	■		■	▲	△	▲	■	▲	▲	▲	■

■	▲	▲	▲	■	▲	▲	▲	■		■	△	▲	▲	■	△	▲	▲	■

Table 2: Representation of a full and reduced kinematics models. Terms u_{x2}^2, u_{y4}^1, u_{z3}^1, u_{x2}^2, Φ_1^1, Φ_1^2 terms are deactivated.

z	$u_x \times 10^{12}$, [m]		Φ, [V]		$\sigma_{zz} \times 10$, [Pa]		$\mathcal{D}_z \times 10^{13}$, [C/m²]	
	3D [26]	L4	3D [26]	L4	3D [26]	L4	3D [26]	L4
0.500	-47.549	-47.552	0.0000	0.0000	10.000	10.000	160.58	160.58
0.475	-41.425	-41.428	0.0189	0.0189	9.9657	9.9657	149.35	149.35
0.450	-35.424	-35.427	0.0358	0.0352	9.8682	9.8683	117.23	117.23
0.425	-29.531	-29.533	0.0488	0.0488	9.7154	9.7155	66.568	66.566
0.400	-23.732	-23.733	0.0598	0.0599	9.5151	9.5153	-0.3382	-0.3348
0.300	-10.480	-10.477	0.0589	0.0590	8.5199	8.5196	-0.1276	-0.1277
0.200	0.1413	0.1411	0.0589	0.0589	7.3747	7.3757	0.0813	0.0813
0.100	9.8917	9.8880	0.0596	0.0596	6.1686	6.1678	0.2913	0.2914
0.000	20.392	20.394	0.0611	0.0611	4.9831	4.9855	0.5052	0.5053
-0.100	24.768	24.771	0.0634	0.0634	3.8045	3.8052	0.7259	0.7261
-0.200	29.110	21.291	0.0665	0.0666	2.6137	2.6131	0.9563	0.9565
-0.300	33.819	33.822	0.0706	0.0706	1.4821	1.4823	1.1995	1.1997
-0.400	39.309	39.313	0.0756	0.0756	0.4868	0.4867	1.4587	1.4590
-0.425	44.492	44.495	0.0602	0.0602	0.2845	0.2844	-58.352	-58.350
-0.450	49.772	49.776	0.0425	0.0425	0.1312	0.1311	-103.66	-103.67
-0.475	55.163	55.167	0.0224	0.0225	0.0340	0.0340	-132.40	-132.40
-0.500	60.678	60.682	0.0000	0.0000	0.0000	0.0000	-142.46	-142.46

Table 3: Piezo-mechanic static response of a piezoelectric plate. Analytical solution from [26] for sensor configuration - $a/h = 4$. Material properties reported in [26].

z	$u_x \times 10^{12}, [m]$		$\Phi, [V]$		$\sigma_{zz} \times 10^3, [Pa]$		$\sigma_{xz} \times 10^3, [Pa]$	
	3D [26]	L4	3D [26]	L4	3D [26]	L4	3D [26]	L4
0.500	-32.764	-32.765	1.0000	1.0000	0.0000	0.0000	0.0000	0.0000
0.475	-23.349	-23.350	0.9971	0.9972	-0.8333	-0.8300	41.457	41.457
0.450	-13.973	-13.974	0.9950	0.9951	-2.8471	-2.8399	64.626	64.629
0.425	-4.6174	-4.6180	0.9936	0.9936	-5.3241	-5.3140	69.556	69.558
0.400	4.7356	4.7352	0.9929	0.9931	-7.5482	-7.5339	56.259	56.034
0.300	2.9808	2.9801	0.8415	0.8416	-12.957	-12.927	19.082	19.152
0.200	1.7346	1.7346	0.7014	0.7015	-15.245	-15.260	-4.5693	-4.6376
0.100	0.8008	0.8014	0.5707	0.5708	-15.510	-15.479	-18.203	-18.130
0.000	0.0295	0.0297	0.4476	0.4477	-14.612	-14.629	-23.866	-23.863
-0.100	-0.4404	-0.4401	0.3305	0.3306	-12.524	-12.512	-25.282	-25.271
-0.200	-0.8815	-0.8811	0.2179	0.2179	-9.2558	-9.2602	-25.633	-25.625
-0.300	-1.3206	-1.3202	0.1081	0.1082	-5.5018	-5.4906	-24.994	-24.984
-0.400	-1.7839	-1.7834	-0.0010	-0.0010	-1.8733	-1.8958	-23.379	-23.376
-0.425	-2.0470	-2.0464	-0.0009	-0.0010	-1.1074	-1.1066	-18.888	-18.881
-0.450	-2.3140	-2.3134	-0.0008	-0.0008	-0.5162	-0.5157	-13.501	-13.497
-0.475	-2.5856	-2.5849	-0.0004	-0.0004	-0.1351	-0.1350	-7.2092	-7.2064
-0.500	-2.8625	-2.8618	0.0000	0.0000	0.0000	0.0000	0.0000	0.0000

Table 4: Piezo-mechanic static response of a piezoelectric plate. Analytical solution from [26] for actuator configuration - $a/h = 4$. Material properties reported in [26].

	$a/h = 4$			$a/h = 100$		
z	$u_z \times 10^{10}, [m]$	$\Phi \times 10^2, [V/m]$	$\sigma_{zz}, [Pa]$	$u_z \times 10^4, [m]$	$\Phi, [V/m]$	$\sigma_{zz}, [Pa]$
	L4					
-0.5	0.8141	0.0000	0.0000	0.2640	0.0000	0.0000
-0.4	0.8331	0.4239	0.0262	0.2641	2.5932	0.0258
0.0	0.8683	0.3261	0.4969	0.2641	2.5921	0.5000
0.4	0.8654	0.2937	0.9733	0.2641	2.5918	0.9742
0.5	0.8555	0.0000	1.0000	0.2640	0.0000	1.0000
	E4					
-0.5	0.8138	0.0000	0.0170	0.2639	0.0000	27.896
-0.4	0.8321	0.4148	0.2179	0.2639	2.5486	-87.572
0.0	0.8676	0.3197	0.4836	0.2639	2.5475	0.4861
0.4	0.8648	0.2887	1.0381	0.2639	2.5472	88.496
0.5	0.8551	0.0000	0.9689	0.2639	0.0000	-26.914

Table 5: Piezo-mechanic static response of a square isotropic plate, problem 1.

	$a/h = 4$			$a/h = 100$		
z	$u_z \times 10^{11}, [m]$	$\Phi, [V/m]$	$\sigma_{zz} \times 10^3, [Pa]$	$u_z \times 10^{11}, [m]$	$\Phi, [V/m]$	$\sigma_{zz} \times 10^6, [Pa]$
	L4					
-0.5	-0.7727	0.0000	0.0000	-0.7661	0.0000	0.0000
-0.4	-0.7860	-0.2064×10^{-3}	-1.6864	-0.7673	0.7935×10^{-4}	0.0946
0.0	-0.7951	0.4515	-25.20	-0.7677	0.4999	0.4275
0.4	-0.7456	0.9938	-11.80	-0.7679	0.9999	0.0681
0.5	-0.9832	1.0000	0.0000	-0.7695	1.0000	0.0000
	E4					
-0.5	-0.5850	0.0000	1.5962	-0.7677	0.0000	0.0000
-0.4	-0.5489	0.7020×10^{-3}	-0.1925	-0.7689	0.7929×10^{-4}	0.0943
0.0	-0.6458	0.4523	0.5030	-0.7692	0.4999	0.4259
0.4	-0.5630	0.9947	-1.2224	-0.7695	0.9999	0.6770
0.5	-0.7633	1.0000	1.8722	-0.7710	1.0000	0.0000

Table 6: Piezo-mechanic static response of a square isotropic plate, problem 2.

a/h	4	100
	Problem 1	
	$M_e : 27/28$	$M_e : 9/28$
u_z		
	Problem 2	
	$M_e : 27/28$	$M_e : 4/28$
Φ		

Table 7: Reduced E4 models, isotropic plate.

a/h	4	100
	$M_e : 19/52$	$M_e : 17/52$
u_z		
	$M_e : 24/52$	$M_e : 19/52$
σ_{xx}		
	$M_e : 20/52$	$M_e : 18/52$
σ_{xz}		
	$M_e : 20/52$	$M_e : 18/52$
σ_{yz}		
	$M_e : 18/52$	$M_e : 18/52$
σ_{zz}		
	$M_e : 20/52$	$M_e : 17/52$
Φ		
	$M_e : 26/52$	$M_e : 22/52$
COMBINED		

Table 8: Reduced L4 model for isotropic plate - problem 1.

a/h	4	100
	$M_e : 25/52$	$M_e : 19/52$
u_z		
	$M_e : 26/52$	$M_e : 19/52$
σ_{xx}		
	$M_e : 24/52$	$M_e : 21/52$
σ_{xz}		
	$M_e : 24/52$	$M_e : 21/52$
σ_{yz}		
	$M_e : 23/52$	$M_e : 21/52$
σ_{zz}		
	$M_e : 17/52$	$M_e : 16/52$
Φ		
	$M_e : 31/52$	$M_e : 25/52$
COMBINED		

Table 9: Reduced L4 model for isotropic plate - problem 2.

	a/h = 4			a/h = 100		
z	$u_z \times 10^9, [m]$	$\Phi \times 10^2, [V/m]$	$\sigma_{zz}, [Pa]$	$u_z \times 10^4, [m]$	$\Phi, [V/m]$	$\sigma_{zz}, [Pa]$
	L4					
-0.5	0.2843	0.0000	0.0000	0.4675	0.0000	0.0000
-0.4	0.2877	0.7562	0.0487	0.4675	4.5821	0.0457
0.0	0.3003	0.6109	0.4982	0.4675	4.5804	0.5000
0.4	0.3176	0.5985	0.9515	0.4675	4.5802	0.9544
0.5	0.3153	0.0000	1.0000	0.4675	0.0000	1.0000
	E4					
-0.5	0.2707	0.0000	0.1608	0.4673	0.0000	29.052
-0.4	0.2741	0.7831	0.0519	0.4674	4.5709	-42.987
0.0	0.2859	0.6128	0.5482	0.4674	4.5690	-12.572
0.4	0.3005	0.5758	3.3692	0.4674	4.5686	-19.560
0.5	0.2985	0.0000	-0.7427	0.4673	0.0000	-29.649

Table 10: Piezo-mechanic static response of a square laminated plate, problem 1.

z	$a/h=4$			$a/h=100$		
	$u_z \times 10^{11}, [m]$	$\Phi, [V/m]$	$\sigma_{zz} \times 10^3, [Pa]$	$u_z \times 10^{11}, [m]$	$\Phi, [V/m]$	$\sigma_{zz} \times 10^6, [Pa]$
L4						
-0.5	-1.4246	0.000	0.0000	-1.3432	0.0000	0.0000
-0.4	-1.4415	-1.0391×10^{-4}	-1.8958	-1.3471	2.3089×10^{-4}	0.2152
0.0	-1.4707	0.4477	-14.629	-1.3493	0.4999	1.0592
0.4	-1.3955	0.9929	-7.5339	-1.3514	0.9998	0.2002
0.5	-1.6058	1.0000	0.0000	-1.3556	1.0000	0.0000
z	$u_z \times 10^{11}, [m]$	$\Phi, [V/m]$	$\sigma_{zz}, [Pa]$	$u_z \times 10^{11}, [m]$	$\Phi, [V/m]$	$\sigma_{zz} \times 10^3, [Pa]$
E4						
-0.5	-3.3720	0.0000	0.9952	-3.2203	0.000	-7.1137
-0.4	-3.4004	-4.5484×10^{-4}	-0.6361	-3.2240	2.3272×10^{-4}	12.091
0.0	-3.5675	0.4481	0.0679	-3.2282	0.4999	0.8525
0.4	-3.2947	0.9942	-0.0156	-3.2317	0.9998	-3.5903
0.5	-3.5348	1.0000	1.4086	-3.2358	1.0000	-6.5019

Table 11: Piezo-mechanic static response of a square laminated plate, problem 2.

a/h	4	100
	Problem 1	
u_z	$M_e : 32/32$	$M_e : 13/32$

Problem 2

| Φ | $M_e : 29/32$ | $M_e : 5/32$ |
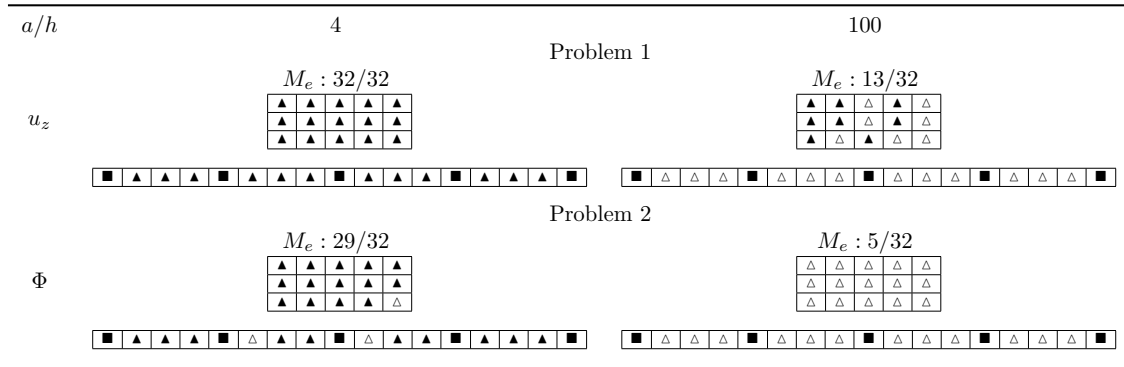
Table 12: Reduced E4 models for laminated plate.
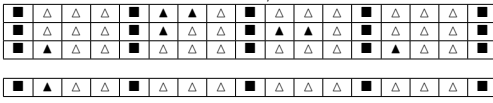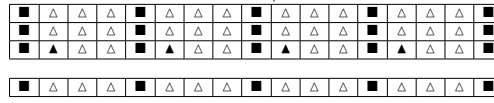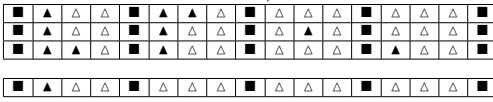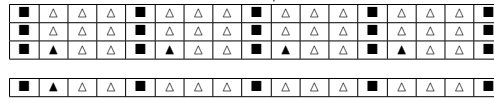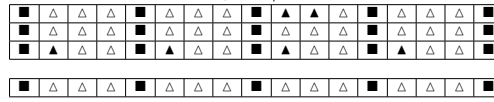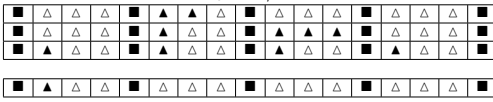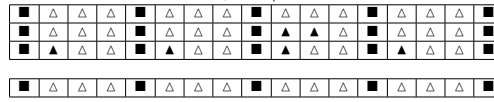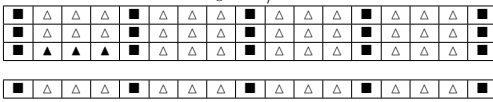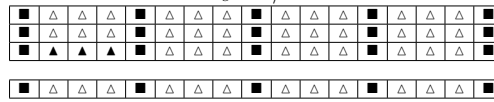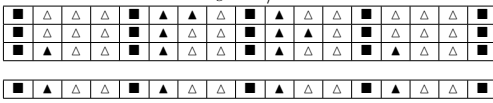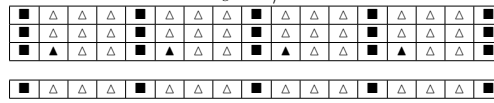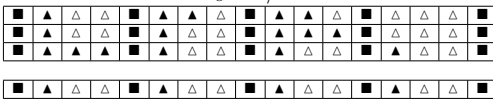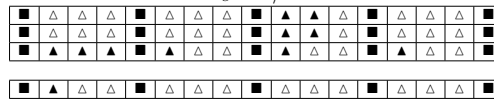
a/h	4	100

u_z — $M_e : 28/68$; $M_e : 24/68$

σ_{xx} — $M_e : 31/68$; $M_e : 25/68$

σ_{xz} — $M_e : 32/68$; $M_e : 26/68$

σ_{yz} — $M_e : 31/68$; $M_e : 26/68$

σ_{zz} — $M_e : 23/68$; $M_e : 23/68$

Φ — $M_e : 34/68$; $M_e : 24/68$

COMBINED — $M_e : 40/68$; $M_e : 31/68$

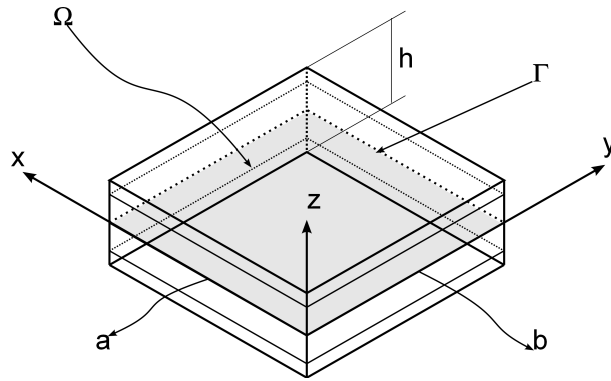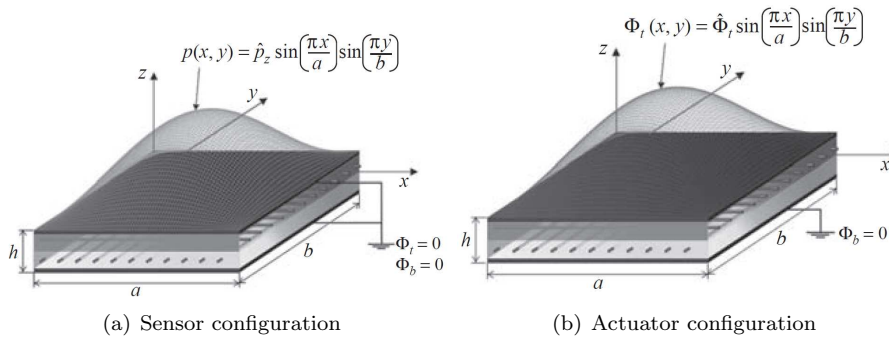Table 13: Reduced L4 model for laminated plate - problem 1.
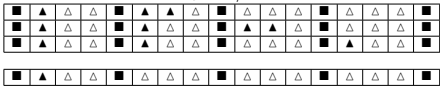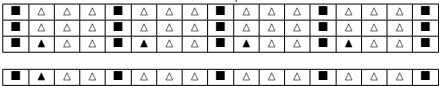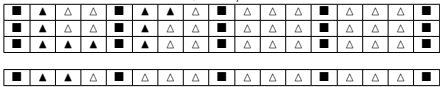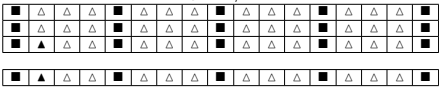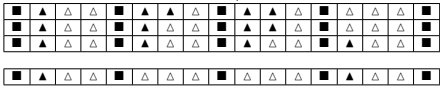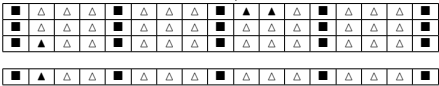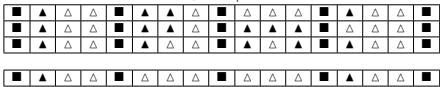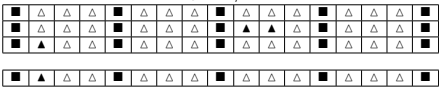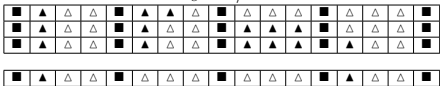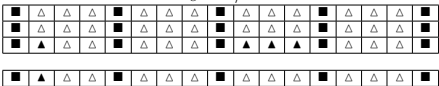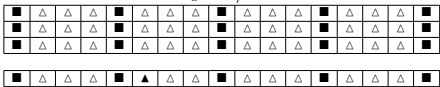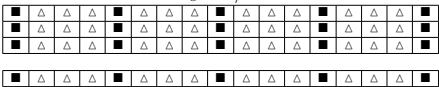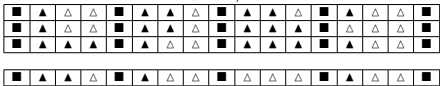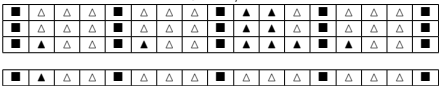
a/h	4	100
	$M_e : 31/68$	$M_e : 25/68$
u_z		
	$M_e : 31/68$	$M_e : 22/68$
σ_{xx}		
	$M_e : 35/68$	$M_e : 24/68$
σ_{xz}		
	$M_e : 37/68$	$M_e : 24/68$
σ_{yz}		
	$M_e : 36/68$	$M_e : 24/68$
σ_{zz}		
	$M_e : 20/68$	$M_e : 20/68$
Φ		
	$M_e : 44/68$	$M_e : 31/68$
COMBINED		

Table 14: Reduced L4 model for laminated plate - problem 2.

Figures

Figure 1: Plate geometry and notations. Piezoelectric configuration: actuator and sensor.

(a) Sensor configuration

(b) Actuator configuration

Figure 2: Piezoelectric plate configuration: actuator and sensor.
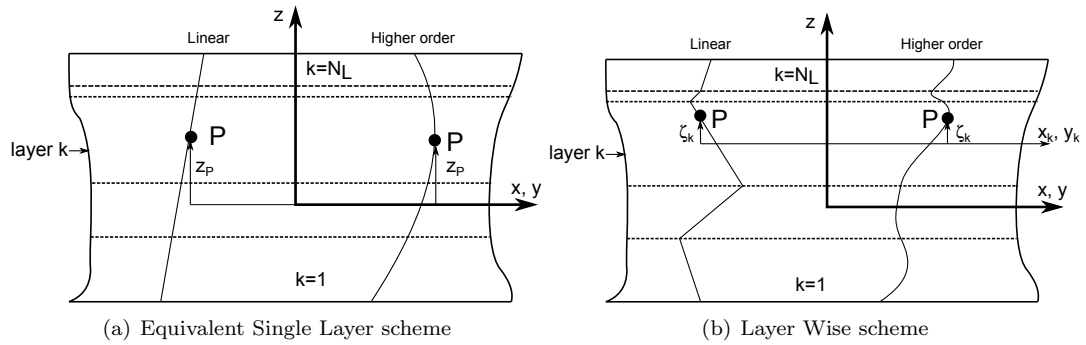
(a) Equivalent Single Layer scheme

(b) Layer Wise scheme

Figure 3: Linear and higher order ESL and LW examples.

22

(a) Isotropic plate
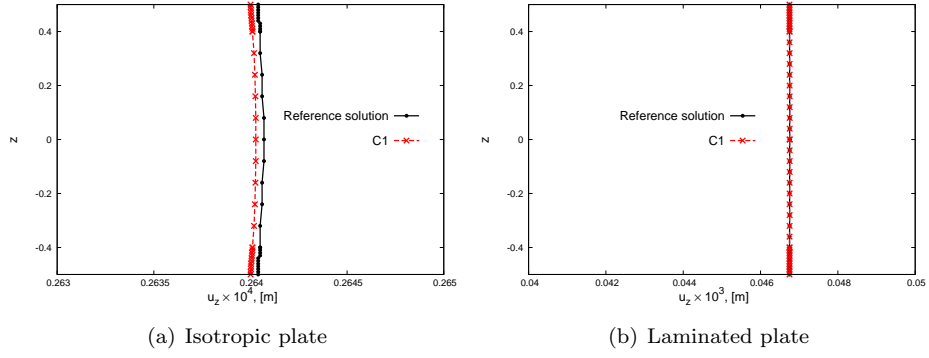
(b) Laminated plate

Figure 4: Displacement u_z vs z evaluated by means of E4 reduced model for isotropic and laminated plate, $a/h = 100$ - problem 1.
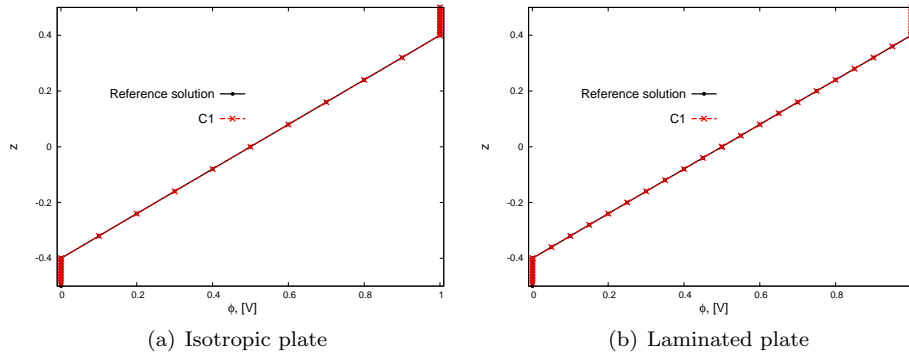
(a) Isotropic plate

(b) Laminated plate

Figure 5: Potential Φ vs z evaluated by means of E4 reduced model for isotropic and laminated plate, $a/h = 100$ - problem 2.

(a) σ_{zz} vs z , $a/h = 4$

(b) Φ vs z, $a/h = 4$

(c) σ_{zz} vs z, $a/h = 100$
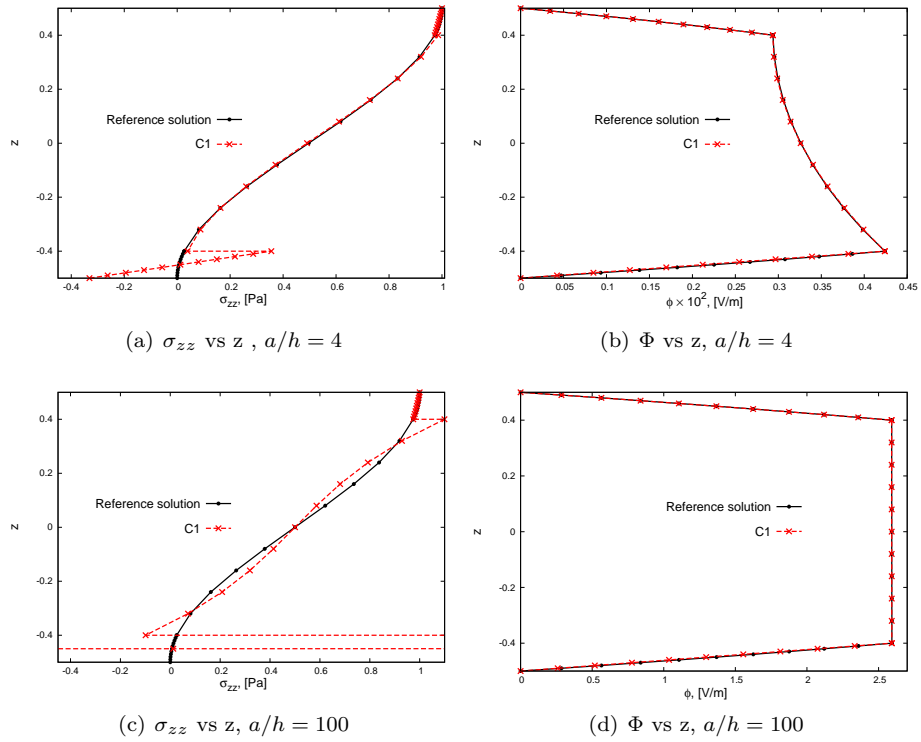
(d) Φ vs z, $a/h = 100$

Figure 6: L4 reduced model for isotropic plate - problem 1.

23

(a) u_z vs z , $a/h = 4$

(b) u_z, $a/h = 100$

(c) σ_{zz} vs z , $a/h = 4$
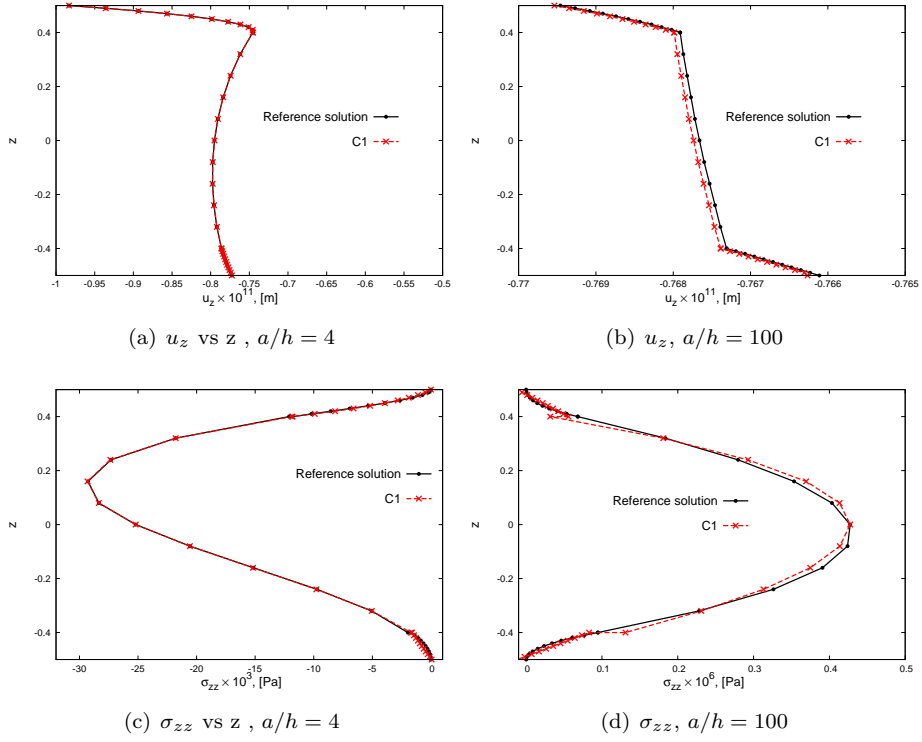
(d) σ_{zz}, $a/h = 100$

Figure 7: L4 reduced model for isotropic plate - problem 2.

(a) σ_{zz} vs z, $a/h = 4$

(b) Φ vs z, $a/h = 4$

(c) σ_{zz} vs z, $a/h = 100$

(d) Φ vs z, $a/h = 100$
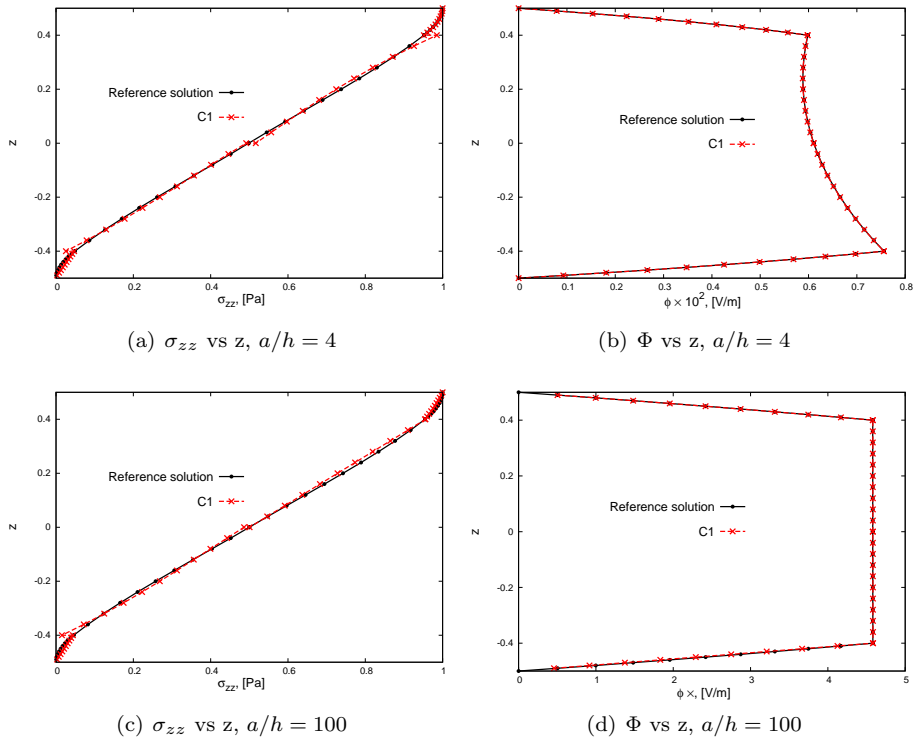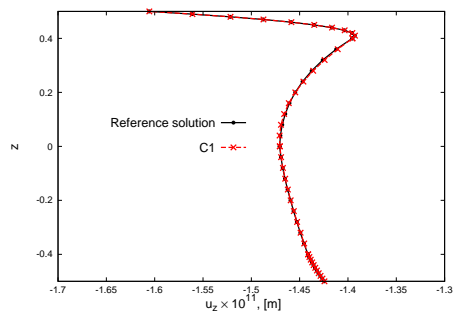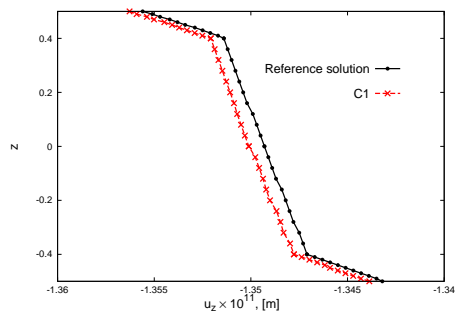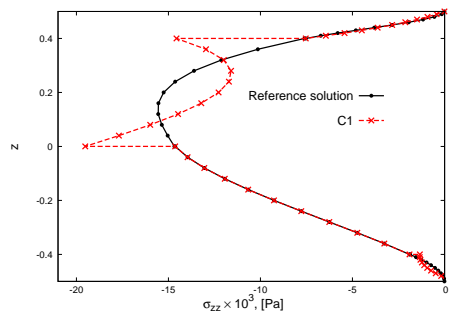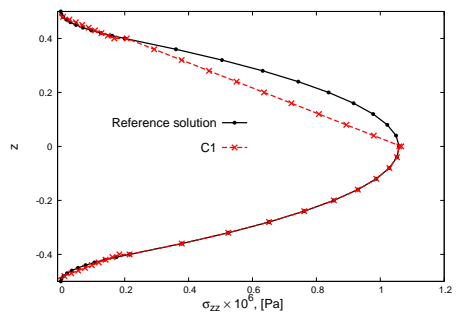
Figure 8: L4 reduced model for laminated plate - problem 1.

(a) u_z vs z , $a/h = 4$

(b) u_z, $a/h = 100$

(c) σ_{zz} vs z , $a/h = 4$

(d) σ_{zz}, $a/h = 100$

Figure 9: L4 reduced model for laminated plate - problem 2.